A gravity wave analysis near to the Andes Range as detected from GPS radio occultation data and mesoscale numerical simulations

A. de la Torre (1) , P. Alexander (1), P. Llamedo (1), D. Luna (1), T. Schmidt (2) and J. Wickert (2)
delatorr@df.uba.ar
(1) Grupo de Dinámica de la Atmósfera, Universidad de Buenos Aires, Buenos Aires, Argentina
(2) GeoForschungsZentrum, Potsdam, Germany

Global maps of potential wave energy per unit mass, recently performed with the Global Positioning System (GPS) Radio Occultation (RO) technique and different satellite missions (CHAMP since 2001, GRACE and COSMIC since 2006) revealed in Argentina, at the eastern side of the highest Andes Mountains, a considerable wave activity in comparison with other extra-tropical regions. The main gravity wave (GW) sources in this natural laboratory are deep convection, topographic forcing and geostrophic adjustment .

The mesoscale numerical model WRF (Weather Research and Forecasting) was used to simulate the atmospheric parameters during representative RO events showing an apparent intense WA in this region. The significance of the relative position of the RO lines of sight, line of tangent points and gravity wave phase surfaces during each event is discussed in relation with the apparent wave activity detected. We also discuss the relative contribution of high and medium intrinsic frequency mountain waves regularly observed, coexisting with inertio gravity waves (IGW), their origin and propagation

♦ The Argentine Mendoza region (70-65W, 30-40S) constitutes a natural laboratory where the main sources of gravity waves (GW) coexist.

♦ The GPS-RO (Global Positioning System Radio Occultation) technique provides valuable information about GW and their properties throughout the atmosphere. This method provides a global coverage, sub-Kelvin temperature accuracy, high vertical resolutions and long-term stability [see, e.g., Wickert et al, 2008 and references therein].

♦ Usually, GW activity has been quantified from GPS-RO temperature profiles, by calculating the mean potential energy through the relative temperature variance content in a vertical column of air σ. For example, in de la Torre and Alexander [2005], this column was selected at a height between Z_1 and Z_2 equal to 19 and 27 km:

$$E_P = \frac{g^2}{2N^2}\sigma\ ;$$

$$\sigma = \frac{1}{(z_2 - z_1)}\int_{z_1}^{z_2}\left(\frac{\delta T}{T_B}\right)^2 dz$$

δT: Band-pass filtered T perturbations between cutoffs at 3 and 9 km.
T_B: Background T
g: Gravitational acceleration
N: Buoyancy frequency

♦ In the Southern Hemisphere, there are extratropical regions that exhibit a strong wave activity close to the Andes and to the Antarctic Peninsula which have been studied with limb sounding techniques [e.g., Jiang et al., 2002, Baumgaertner and McDonald (2007), Alexander et al (2008)].

♦ de la Torre et al. [2006] performed an analysis of the global distribution of gravity wave activity (WA) in the upper troposphere and lower stratosphere between June 2001 and March 2006, using GPS-RO temperature profiles retrieved from the CHAMP satellite. A significant WA with respect to other extra-tropical regions in the Southern Hemisphere was detected in Mendoza, on the eastern side of the highest Andes mountains.

♦ We selected two events taking place in this location, showing intense WA. In order to evaluate the capability of the RO technique to quantify WA, we performed numerical simulations in both cases.

WRF Simulations

We performed simulations with the WRF version 2.1.2 model during two RO events showing a considerably intense WA:
- 30 Aug 2001, 04:10 UTC
- 20 Nov 2001, 03:58 UTC;

hereinafter S1 and S2 respectively.

We employed three nested domains with horizontal grid spacing of 36, 12, and 4 km respectively, and a time step equal to 30 s.

The inner domains including the topography are shown in Figure 1. The experiments were driven by assimilating lateral boundary conditions and sea surface temperatures from NCEP (National Centers for Environmental Prediction) reanalysis.

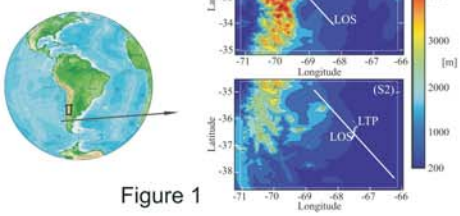

Figure 1

♦ To study δT and the zonal, meridional and vertical velocity perturbations, δU, δV and δW, we first removed the background wind by employing a 2D filtering technique. A 10 - 550 km 2D band pass filter was applied to T, U, V and W, at each constant pressure level and time step.

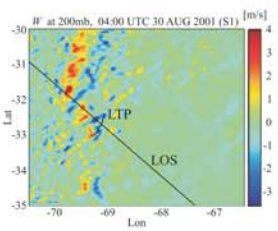

Figure 2

♦ δW is recognized as an indicator of the presence of mountain wave activity. Figure 2 shows δW at 200 mb and the time output closest to each RO event. simulations reveal stationary mesoscale waves above the highest tops, as well as constant phase surfaces quite parallel to the topography, suggesting their orographic origin. It is interesting to note that, even considering that RO temperature profiles reveal important WA for both events, the simulations evidence strong/weak W variations (typically associated to mountain WA) in the vicinity of S1/S2 LTP.

♦ Possible GW contributions related to deep convection activity during both events were discarded from satellite imagery evidence.

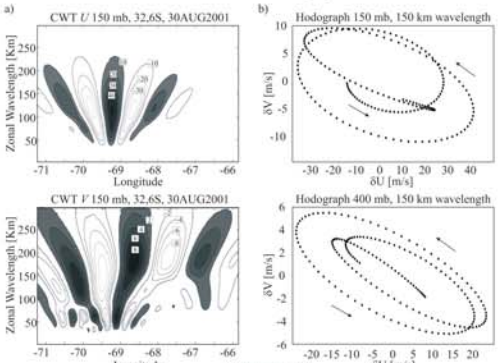

Figure 3

♦ Due to the rapidly varying jet core, long horizontal wave-length IGW radiated by geostrophic adjustment should also be considered. According to this, IGW with downward group velocity below the jet could be expected.

♦ We used continuous wavelet transform (CWT) to analyze wave parameters along different paths, at constant latitude and parallel to the LOS, at different pressure levels and time steps. In every case, we found two principal wave modes. In Figure 3a, we can see the Morlet CWT at constant representative latitudes and pressure level (150 mb) for S1. Similar for S2.

♦ Two principal wave components are seen, both in δU and δV, roughly between λ_{x1} = 50 km and λ_{x2} = 200 km, where λ_x is the zonal wavelength.

♦ Figure 3b shows the hodograph above and below the jet for λ_x=150 km component (S1), rotate counter-clockwise eastwards at constant pressure level, evidencing downward phase velocity

♦ The obtained profiles have vertical resolutions progressively increasing from 0.5 km in the troposphere up to 1.4 km in the lower stratosphere [Kursinsky et al., 1997] and a horizontal resolution of 150 km along each line of sight (LOS). The perigee of the LOS between satellites projected on the Earth's surface determines the geographical coordinates where the atmospheric parameters are given. Successive perigees during the occultation form the line of tangent points (LTP) (Figure 4, left).

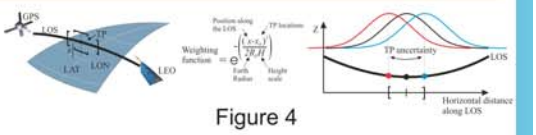

Figure 4

♦ The RO bending angle is an integrated measure of the refractive index (and therefore temperature) in the atmosphere traversed by the optical ray. The contribution of the index to the integral peaks at the perigee and decays exponentially away from it [Preusse et al., 2002] (Figure 4, center).

♦ There is an uncertainty in the determination of the exact position of each tangent point (TP) in geographical coordinates. TPs may be displaced away from the perigee along each ray path, between +/- 25 km and +/- 50km in the 10-16km and 16-35 km altitude intervals respectively [Liou et al., 2007] (Figure 4, left and right). The peak of the exponential decay does not always coincide with each TP. This affects the horizontal resolution. A given RO may reveal a vertical temperature profile evidencing an apparent larger (or nonexistent) WA at the perigees. This is the case in S2 (Figure 5, right), where each LOS penetrates a wave packet far away from its corresponding TP.

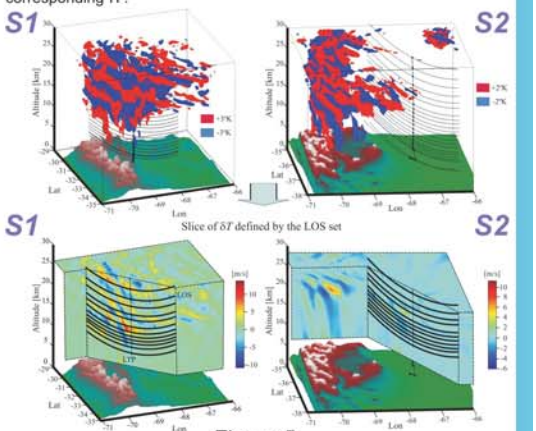

Figure 5

♦ We must be careful when we interpret the atmospheric region where a given RO event predicts intense WA. Figure 5 (upper) shows the 3D contours corresponding to δT = ±3 K, for S1 and δT = ±2K for S2. This plot includes LTPs and LOSs. Figure 5 (bottom) shows δT at the vertical cross section defined by the set of LOSs. Wave phase surfaces tilt westward, evidencing a downward-westward phase progression clearly corresponding to MWs. Optical ray paths in the cross section are also shown.

♦ A first insight shows an intense WA in S1 close to the tangent points (as predicted by the corresponding RO), whereas for S2, there are only weak wave packets in the troposphere, approximately 100 km away from the tangent points. Note in Figure 5 for S2, the partial penetration of LOSs into the high wave amplitude atmospheric region. From these two examples, in addition to the systematic GPS-RO uncertainties mentioned above, a question arises: are these measurements adequate to quantify WA of single events?

References

Alexander, M.J. et al. (2008), Global Estimates of Gravity Wave Momentum Flux from High Resolution Dynamics Limb Sounder (HIRDLS) Observations, J. Geophys. Res., 113, D15S18, doi:10.1029/2007JD008807.
Baumgaertner, A. J. G., and A. J. McDonald (2007), A gravity wave climatology for Antarctica compiled from Challenging Minisatellite Payload/Global Positioning System (CHAMP/GPS) radio occultations, J. Geophys. Res., 112, D05103, Doi:10.1029/2006JD007504.
de la Torre, A. and P. Alexander (2005), Gravity waves above Andes detected from GPS radio occultation temperature profiles: Mountain forcing?, Geophys. Res. Lett., 32, L17815, doi:10.1029/2005GL022959.
de la Torre, A., T. Schmidt and J. Wickert (2006), A global analysis of wave potential energy in the lower stratosphere derived from 5 years of GPS radio occultation data with CHAMP, Geophys.Res.Lett., 33, L24809, doi:10.1029/2006GL027696.
Jiang, J.H. et al. (2002), Upper Atmosphere Research Satellite (UARS) MLS observation of mountain waves over the Andes, J. Geophys. Res., 107, 8273, doi:10.1029/2002JD002091.
Kursinski, E. R. et al. (1997), Observing Earth's atmosphere with radio occultation measurement using the Global Positioning System, J. Geophys. Res., 102, 429-465.
Liou, Y.A. et al. (2007), FORMOSAT-3/COSMIC GPS Radio Occultation Mission: Preliminary Results, IEEE Trans. Geo. Rem. Sens., 45, 3813-3826.
Preusse, P. et al. (2002), Space-based measurements of stratospheric mountain waves by CRISTA 1. Sensitivity, analysis method, and a case study, J. Geophys. Res., 107, 8178, doi:10.1029/2001JD000699
Wickert, J. et al (2008), GPS radio occultation: Results from CHAMP, GRACE and FORMOSAT-3/COSMIC. Terrestrial, Atmospheric and Oceanic Sciences, in press.

Concluding remarks

After examining WRF results for two selected cases in the vicinity of the RO LTP, we found intense activity only near to the mountains.

A wavelet analysis led us to identify two principal modes of oscillation with horizontal wavelengths between 50 and 200 km, both clearly corresponding to mountain waves.

A hodograph for the longest wave shows downward phase velocity at all heights of the simulation. This evidences that IGW do not stem from geostrophic adjustment at jet levels, but from topographic forcing.

We observe that one of the simulations does not show intense WA in the vicinity of the tangent points, even though the GPS-RO temperature profile detects it.

The GPS-RO technique may not be by itself reliable enough to quantify and locate WA of single events, nevertheless, it should be considered a very useful tool to observe the global WA in statistical studies.